Phase Tensor Analysis and 2D Modeling of Magnetotelluric Method Data in The Nullarbor Area, South Australia

Sarah Manurung, Andri Yadi Paembonan*, Selvi Misnia Irawati

Geophysical Engineering, Faculty of Industrial Technology, Sumatra Institute of Technology, Lampung 35365, Indonesia

*Corresponding author. Email: andri.paembonan@tg.itera.ac.id

Abstract

Earth's geological structures are generally the result of tectonic processes. This study aims to determine the dimensions and direction of the geoelectric strike based on phase tensor analysis and 2D modeling to determine the subsurface structure in the Nullarbor area, South Australia using the magnetotelluric method. The magnetotelluric method is a passive geophysical technique used to create images of subsurface structures based on variations in rock resistivity. Data was obtained in EDI file mean the data has been processed and convert to apparent resistivity and frequency. Furthermore, data is analysis in the phase tensor process and then identify the Geoelectrical strike direction. Based on the tensor analysis, the results show that the study area has 2D dimensions, and the direction of the geoelectric cross section is from North to South, specifically N5°E. This geoelectric direction corresponds to the regional geological structure. After rotation in this direction, 2D inversion modeling of the MT data shows rock layers consisting of Eucla basins with sediment and volcanics rocks below 10 Ωm and Officer basin contain a sediment rock that has higher resistivity ranging from 10 to about 300 Ωm. Furthermore, the resistive layer with 300 – 2000 Ωm is expected as the upper crust in the central Coompana Province trending granite-rich corridor. This result show that the geological structure and lithology could be identified in this study area by analyzing the phase tensor and from the 2D model.

Keywords: dimensionality; geoelectrical strike; geological structure; inversion; magnetotelluric.

Introduction

Geological investigations into the Earth's layers reveal structures shaped by tectonic processes within a given region. These phenomena stand out as a critical area of study. It occurs when the deformation of rocks leads to displacements between adjacent rock blocks, offering valuable insights into the dynamic forces that shape our planet. The range of displacements can be very wide, ranging from a few millimeters to tens of kilometers, and are often triggered by the movement of tectonic plates, especially in subduction zones. The geological structures can cause earthquakes that cause significant losses. Therefore, the study of geological structure is important to minimize the impact of earthquake losses. The existence of geological structure such as fault not only has negative impacts, such as the potential for earthquakes that can cause significant losses but also has positive benefits. Faults can increase conductivity creating pathways for mineral fluid flow, which has high economic value (Akbar et al., 2020). This research focused on the Nullarbor Plain region of South Australia, which is known as the largest karst plain in the world. The region has an area of approximately 200,000 km² and is covered by thick layers of limestone (Scheib et al., 2016). Significant transformations occur in this region due to linear cracks caused by thrust faults in the

rock structure (Pawley et al., 2020). The Magnetotelluric method was used in this study to understand the subsurface conditions of the earth (Chang et al., 2023; Lin et al., 2023; Pertiwi et al., 2023). This method utilizes variations in the earth's magnetic field to measure subsurface conductivity (Simpson & Bahr, 2005). Measurements are made in the perpendicular direction on the earth's surface to get an overview of the subsurface structure. This method has the advantage of mapping the resistivity distribution in the subsurface (Barajas-Olalde et al., 2023; Marwan et al., 2022).

Previous research in the Nullarbor region has used various methods, including magnetic (Hu et al., 2019; Pawley et al., 2020), gravity (Heath, 2017; Heath et al., 2018) and seismic methods, to understand the role of fluids in seismic activity and the development of tectonic structures (Yang et al., 2022). However, no studies have used phase tensor analysis. In this study, phase tensor analysis is used to identify the type of dimensionality and direction of geoelectrical strike to determine the direction of structure in the study area (Irawati et al., 2024; Maswah et al., 2021). By combining magnetotelluric data with geological information, this study aims to obtain an accurate 2D subsurface model and interpret the lithology and fault structure in the study area. It is expected that the results of this study will provide a deeper understanding of the geology and potential earthquake risk in the Nullarbor Plain and can contribute to the optimization of mineral resource utilization in the area.

Materials and Methods

Geological setting

Nullarbor is a region located on the coast of the Great Australian Bight in South Australia with the Victorian Desert to its north. The region is the largest expanse of limestone in the world with an area of about 200,000 square kilometers or 77,000 square miles. Based on the Geological Map of Nullarbor sourced from the Geological Map of South Australia in 2020 (Figure 1), the overall geology in the study area is dominated by Tertiary rocks (Geological Survey of Western Australia, 2017; Cowley, 2020). The study is located at the Eucla Basin. Its boundary, which spans 2,000 kilometers from Western Australia to South Australia, are a large offshore, nearshore, and onshore province of marine and coastal sediments up to 300 meters thick (Hou et al., 2022). Sedimentary records from the basin and surrounding paleo valleys offer a more comprehensive picture of the region's geological history than only basin deposits.

Sedimentary rocks in Nullarbor are Miocene and Pliocene age, consisting of limestone and marine fossil limestone (Czi). At the end of the early Miocene, the sea retreated for less than 1 million years and then advanced again in the middle Miocene. Nodular algal limestone was deposited in much the same area as the Abrakurrie limestone forming the mulla mullang member of the Nullarbor limestone. Seawater then encroached further across the valley, depositing thin beds of Nullarbor limestone generally less than 20 meters across the Nullarbor area. The origin of this limestone is attributed to the abundance of foraminifera and the relatively high proportion of aragonite components (Webb & James, 2006).

The middle part of the Coompana Province has a two-layer crust. The upper crust is 14-17 km thick and stretches approximately 140 km westward from the Palinar Shear Zone to the Border Shear Zone. The top crust between the Palinar and Bunburra shear zones is plain and lacks reflectors. It correlates to the northeast trending granite-rich corridor (Pawley et al., 2020).

Magnetotelluric Method

The magnetotelluric method is one of the passive geophysical methods used to create

images of subsurface structures based on variations in rock resistivity (Chang et al., 2023; Lin et al., 2023; Pertiwi et al., 2023). This electromagnetic field originates from a variety of very complex physical processes that result in its frequency spectrum having a very wide range ranging from 10^{-5} Hz to 10^4 Hz (Arisbaya et al., 2023). An understanding of the magnetotelluric (MT) method can be obtained by considering the principle of propagation of incident electromagnetic waves. In a mathematical context, the principle of the magnetotelluric method is explained through Maxwell's equations. The relationship between the orthogonal components of the electric field and the horizontal magnetic field is described using the impedance tensor (Z) (Irawati et al., 2024; Maswah et al., 2021).
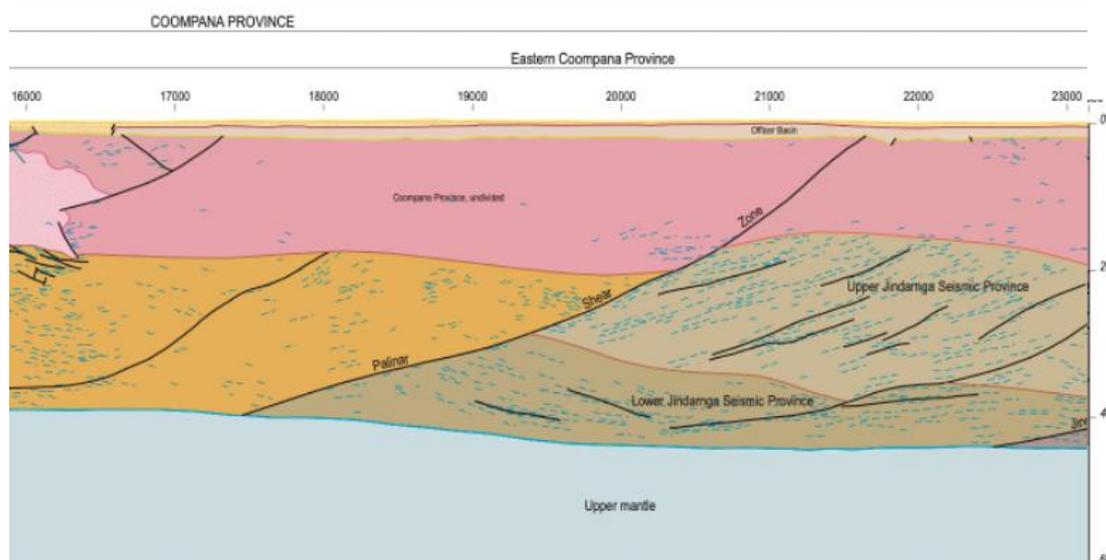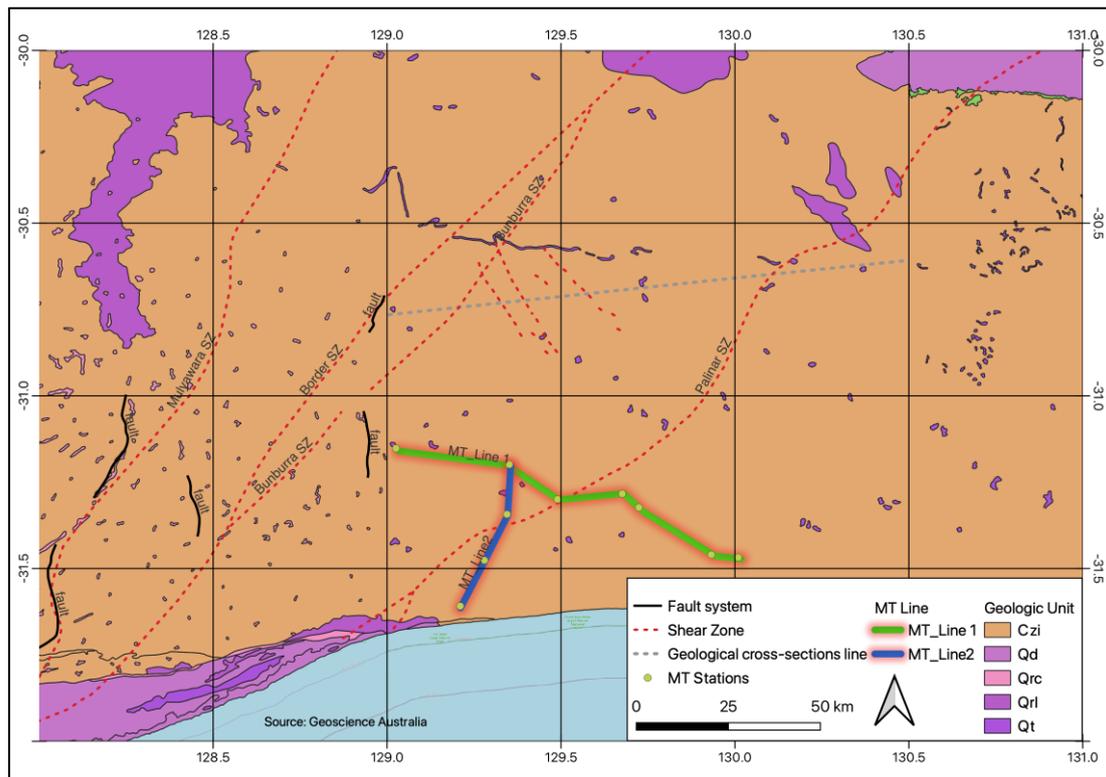
Figure 1. Geologic map (top) showing the fault and fracture zone including magnetotelluric measurements lines at Nullarbor and interpreted geological section (bottom) (Geological Survey of Western Australia, 2017; Cowley, 2020).
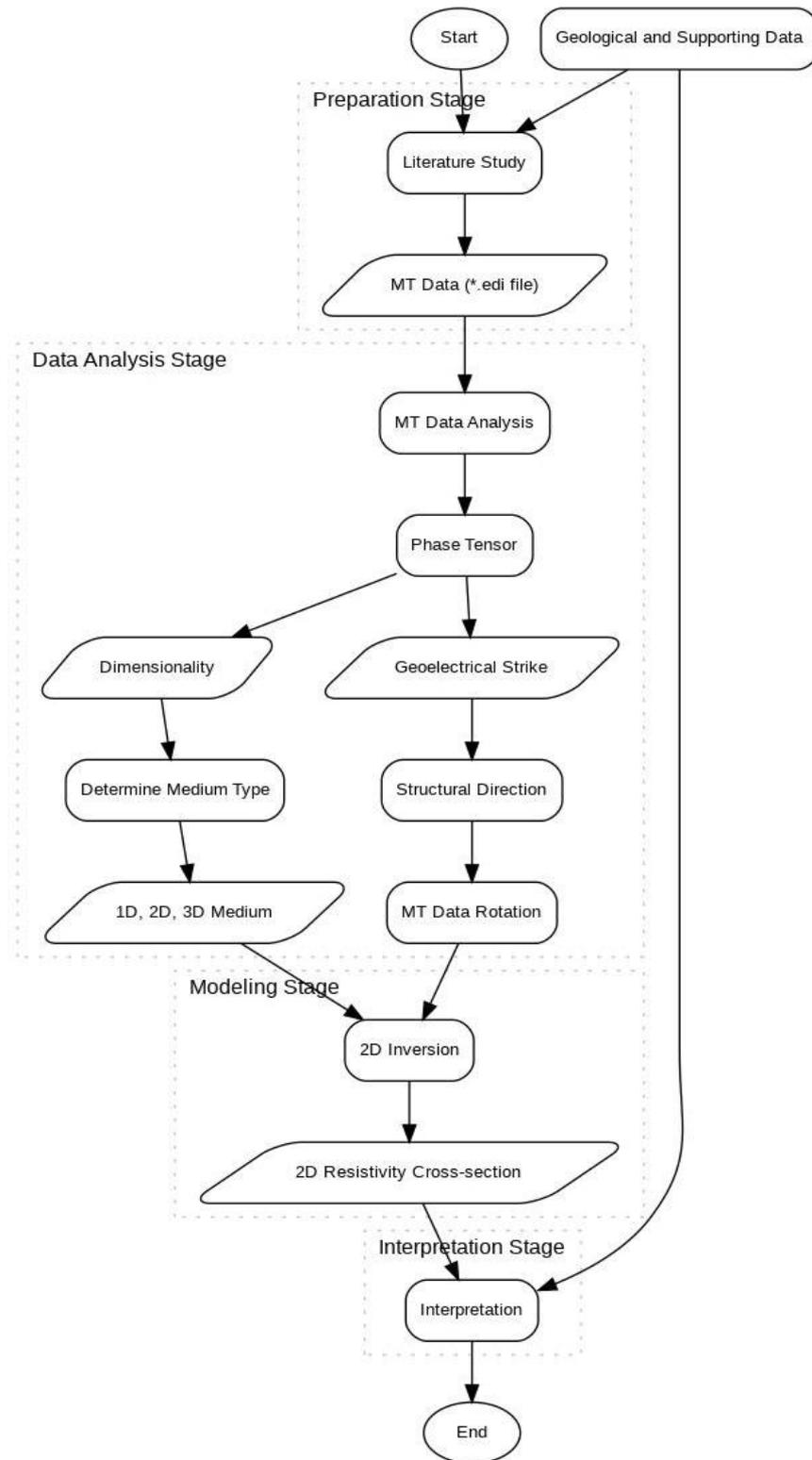
Figure 2. Flow diagram of the MT data processing, analysis, and 2D modeling.

$$E = ZH \tag{1}$$

$$\begin{pmatrix} E_x \\ E_y \end{pmatrix} = \begin{pmatrix} Z_{xx} & Z_{xy} \\ Z_{yx} & Z_{yy} \end{pmatrix} \begin{pmatrix} H_x \\ H_y \end{pmatrix} \tag{2}$$

Where (Z) serves as a transfer function and has the form of a complex number that can

also be expressed as apparent and phase resistivity, as described in equations (1) and (2). Therefore, the apparent and phase resistivity can be explained through the following equations:

$$\rho_\alpha = \frac{1}{\omega\mu_0}|Z|^2 \qquad (3)$$

$$\phi = \tan^{-1}\left[\frac{Im(Z)}{Re(Z)}\right] \qquad (4)$$

According to Bravo-Osuna et al. (2021), the phase (Φ) can be explained as the ratio between the real and imaginary numbers of an impedance tensor complex number. Through the ratio between the real and imaginary numbers, a relationship can be found in the form of a matrix or tensor represented in the following equation:

$$Z = X + iY \qquad (5)$$

$$X^{-1}Y = \begin{bmatrix} \phi_{xx} & \phi_{xy} \\ \phi_{yx} & \phi_{yy} \end{bmatrix} \qquad (6)$$

Data and Processing Steps

This study utilized secondary data obtained from the acquisition of the Magnetotelluric (MT) method in the Nullarbor region, specifically in Coompana province, conducted by the Geoscience Australia (Jiang et al., 2017). Data consists of 14 measurement points presented in *.edi format where the data have been processed and converted to apparent resistivity and phase (Figure 3). Procedure to process and analyze the data is shown in Figure 2. analysis was conducted to determine the geoelectrical strike and dimensionality of the study area. MT data was analyzed using phase tensor analysis to determine the geoelectrical strike and dimensionality in the study area. The geoelectrical strike analysis process uses the Python programming language on the Google Colab platform with Python code developed by the University of Adelaide (Kirkby et al., 2019). This approach is based on the concept of ellipse theory (Bravo-Osuna et al., 2021) which produces information on the dimensionality and direction of the geoelectrical strike in the study area. The geoelectrical strike analysis was obtained through phase tensor calculations using the MTPy code. The resulting geoelectrical strike directions

were then grouped based on low, medium, and high frequency periods, and then represented in the form of a rose diagram. The output of this analysis is an angle which is then used to rotate the MT data. MT modeling is used to describe the subsurface structure in the study area. In this research, the 2D inversion method is used by applying Nonlinear Conjugate Gradient (NLCG) which could simplify an object function (Guo et al., 2020). The modeling results are also associated with the characteristics of the research area. At this stage, modeling of Transverse Electric (TE) mode and Transverse Magnetic (TM) mode is also conducted. The interpretation process involves analyzing the specific gravity through a 2D inversion process by considering the phase tensor. Furthermore, the results of this analysis were correlated with relevant geological data in the study area (Figure 4).

Results and Discussion

MT data analysis is the first step before starting the modeling process. In this research begins with phase tensor analysis, where in dimensionality it is necessary to overlay the ellipse with the geologic sheet and review the Geoelectrical strike by plotting the rose diagram (Figure 5). In this case to determine the direction of the structure and conductivity of the subsurface medium used for MT data rotation to obtain accurate 2D inversion modeling. The period ranges (low, medium, and high).

The phase tensor analysis in Figure 3(a) shows the phase tensor overlay map at a low period of 0.01 s with skew angle values associated with shallow depths because the resulting skew angle values are dominantly close to zero (where the maximum axis is equal to the minimum axis ($\Phi_{max} = \Phi_{min}$)), dominated by white circles, representing a type of 1D dimensionality. Figure 3(b) displays the phase tensor overlay map at a medium period of 1s with skew angle values associated with medium depth

because the resulting skew angle value is dominantly $-3° < \beta < 3°$ where the maximum axis is not equal to the minimum axis ($\Phi_{max} \neq \Phi_{min}$), dominated by elliptical shapes colored faint red and faint blue, representing the type of 2D dimensionality. Figure 3(c) displays the phase tensor overlay map at a medium period of 100s with skew angle values associated with

deep depths because the resulting skew angle values are dominant at $-3° < \beta < 3°$ where the maximum axis is not equal to the minimum axis ($\Phi_{max} \neq \Phi_{min}$), dominated by elliptical shapes that are colored faint red and faint blue, representing a type of 2D dimensionality. Therefore, over all this MT data has 2D dimensionality.
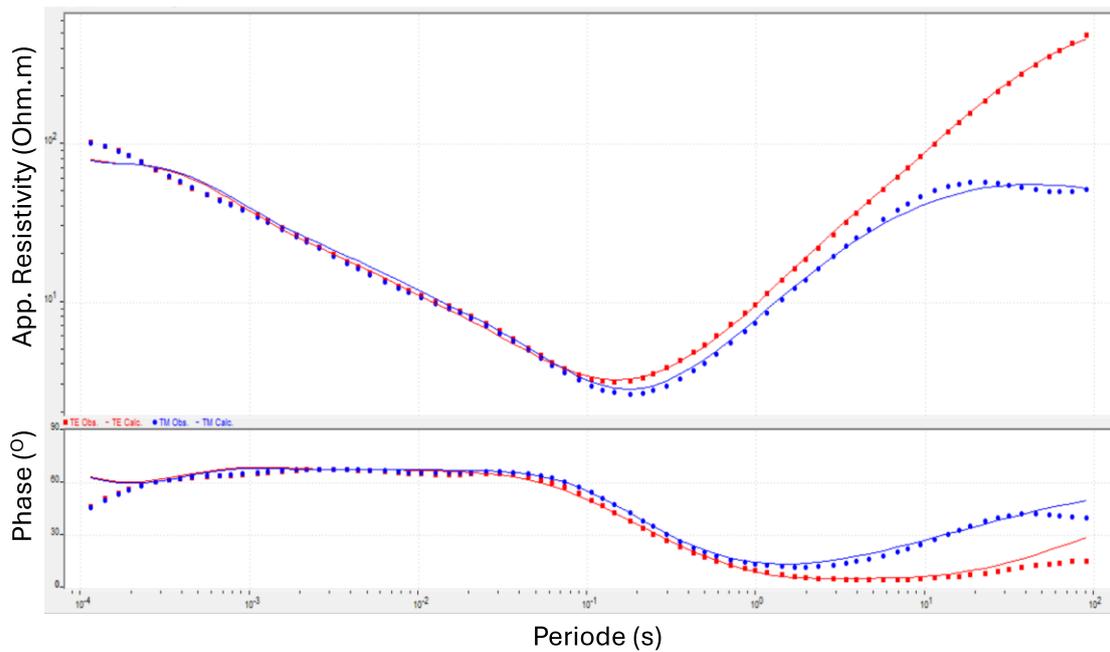

Figure 3. Sample of MT data from the study area, showing both TE (read) and TM (Blue) mode in apparent resistivity (above) and phase (below).
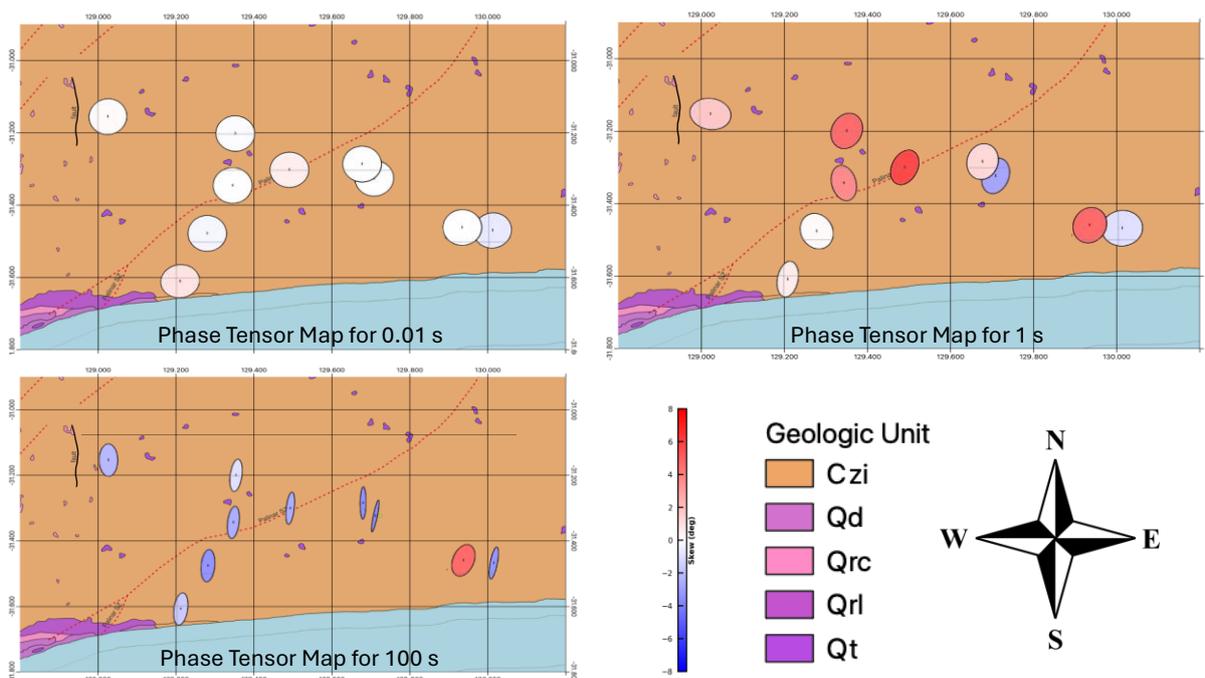

Figure 4. Phase tensor maps of (a) low period (0.01 s), (b) medium period (1 s), and (c) high period (100 s).

In knowing the geoelectric strike direction of the research area that produces the direction of the structure can be visualized with a rose diagram. Geoelectric strike direction in the low period (0.001 - 0.01 s) shows rose diagram Figure 5(a) from phase tensor analysis has an orientation of N75°E. In the medium period (0.1 - 1 s) Figure 5(b) has an orientation of N15°E and N5°E and in the high period (10 - 100 s) has the same orientation of N5°E in Figure 5(c).

(a) **(b)** **(c)**
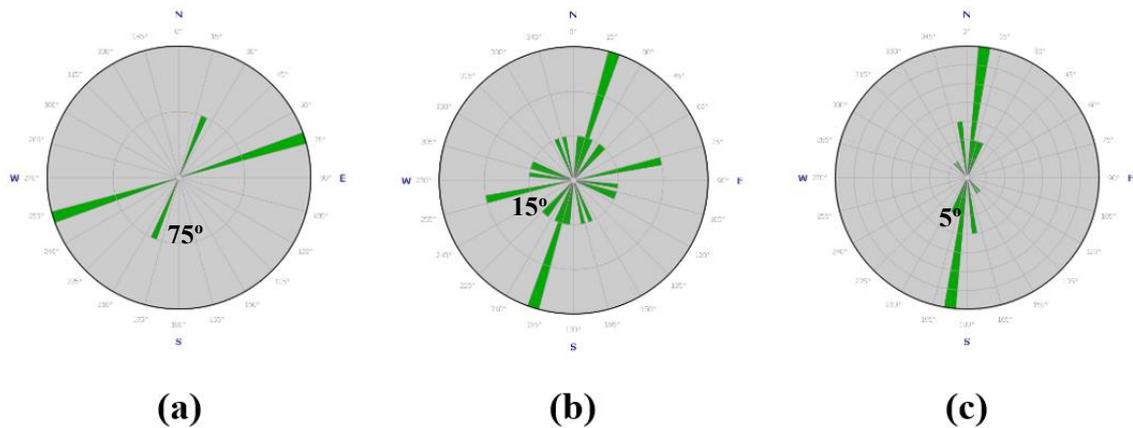
Figure 5. Rose diagram of phase tensor analysis of (A) low period, (B) medium period, and (C) high period.
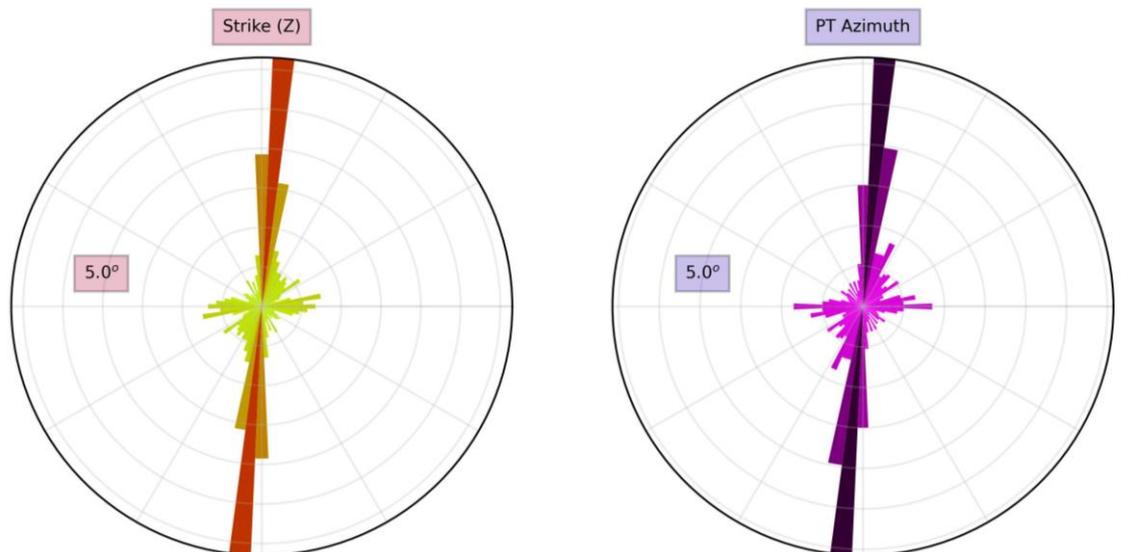
Figure 6. Rose diagrams all periods showing the direction in 5°NS from both strike(left) and phase tensor (right) analysis.

The orientation of the direction found in the high period is N5°E and in all periods also has a dominant orientation of N5°E (Figure 6). Compared to the orientation of the direction of the geological structure in the research area, it is the same as the geoelectrical strike results using a phase tensor of N5°E. The orientation obtained through geoelectrical strike analysis was used to rotate the MT data. A rotation of N5°E was performed to align the data with the regional strike direction before proceeding to the modeling stage. Rotation is necessary in 2D modeling due to the dominance of dimensionality data in this study area by 2D. It aims to ensure the assumption of an infinite elongated structure is met. Thus, the measured geoelectrical strike direction can be aligned with the measurement line because the measurement direction is not always the same as the direction in the modeling.

Based on the phase tensor analysis of all period ranges, it is known that the dominant direction in the MT data of the Nullarbor

area obtained is N5°E and then used to rotate the MT data. Determination of the geoelectric strike direction must have relevance to the geology of the study area, because phase tensor analysis has an ambiguity of 90°. Geoelectric analysis also serves to draw line directions. After the data is rotated and the line is drawn, a 2D inversion is then performed with the Nonlinear Conjugate Gradient (NLCG) approach. This inversion uses a differential function at the minimum function which aims to minimize outliers to produce an optimum model. In this inversion modeling, a combination of TE and TM mode inversion is used. Utilization of TE mode produces good vertical detail (depth) but is less than optimal in displaying lateral layers of the earth. Conversely, TM mode provides good lateral detail but less vertically (depth). Therefore, combining these two modes is necessary to obtain good overall model results both in terms of vertical (depth) and lateral. 2D inversion modeling uses 3 passes where each pass has the same homogeneous initial model with a resistivity of 100 m and has the same iteration treatment of 60 times.

Figure 6 is the result of 2D inversion modeling on line 1 which consists of 7 MT measurement points which are D13, D1, D11, D10, D6, D3, and D9 with a northwest-southeast line direction. In this case using inversion weighting parameters alpha 4, beta 3 and tau 3 produces an RMS error of 1.79%. The 2D model has a depth of 10 km with a line length of 100 km. The resistivity distribution of the model is ranging from 1 to 2000 Ωm. Resistivity values as in Table 1 based on the results of previous research by Jiang et al (2017), Geological Survey of Western Australia (2017), and Pawley et al. (2020). in the South Australia. The resistivity value of Eucla basins consisting of sediment and volcanics rocks below 10 Ωm. Officer basin contain a sediment rock has higher resistivity ranging from 10 to about 300 Ωm. Furthermore, the resistive layer with

300 - 2000 Ωm is expected as the upper crust in the central Coompana Province trending granite-rich corridor.

The existence of geologic structure located in the Nullarbor, especially on line 1, can be suspected using resistivity contrast in 2D inversion modeling. By understanding the different resistivity patterns, especially the contrast between the rocks affected by the structure such as fault or shear zone and the surrounding rocks, we can obtain an indication of the presence and location of the structure. Figure 6 shows the 2D model of line 1, with basin sediment extended to approximately 6 km depth, and bedrock (granite) at >1000 m depth.

Table 1. Rock resistivity in previous studies and drilling results (Geological Survey of Western Australia, 2017).

Lithology	Resistivity (Ωm)
Eucla and Bright Basins consisting of sediment and Vulcanic rocks including Tun formation (Czi)	<10
Office Basin, Sedimentary rock	10-300
Coompana province, undivided (Basement Granite)	300-2000

The geological structures in the Nullarbor area were formed through tectonic activity, sedimentation, and climatic influences. The craton that forms the core of the Nullarbor region is characteristically characterized by a cold and thick lithosphere, providing high rigidity against tectonic deformation. However, neotectonic evidence indicates fault, shear, and fold activity within it, particularly evident in the carbonate rocks (limestones) that form the surface layers of the Nullarbor Plain. The result from the resistivity model line 1 (Figure 6) showing the low resistivity anomaly below 300 Ohm.m in the basement rock, that indicates the shear zone. This could be a part of the Palimar SZ that found in the section of the seismic interpretation in the north.

Figure 7 display 2D modeling on track 2 which consists of 4 MT points which are

D1, D12, D08 and D7 with the direction of the northeast - southwest. In this case using inversion weighting parameters alpha 4, beta 2 and tau 0.3 produces an RMS error of 1.50%. The 2D inversion results have a depth of 10 km with an area of 50 km. The

2D inversion results seen in Figure 7 produce a resistivity distribution in the cross section ranging from a range of 1 - 2000 m.
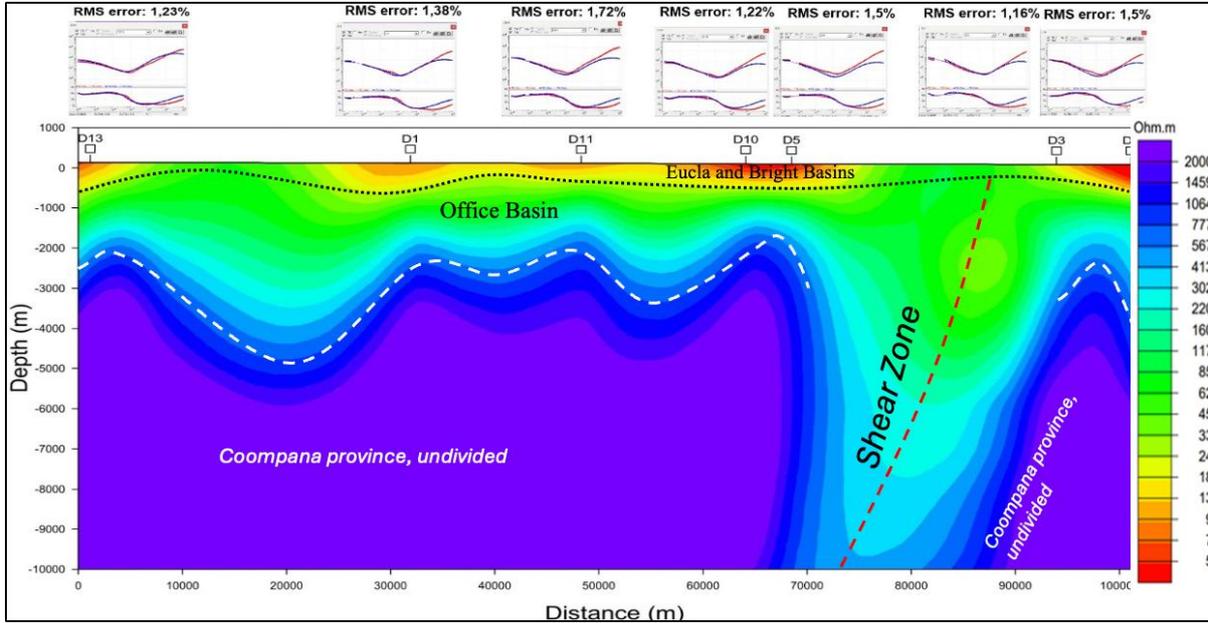

Figure 6. 2D inversion line 1 at Nullarbor.
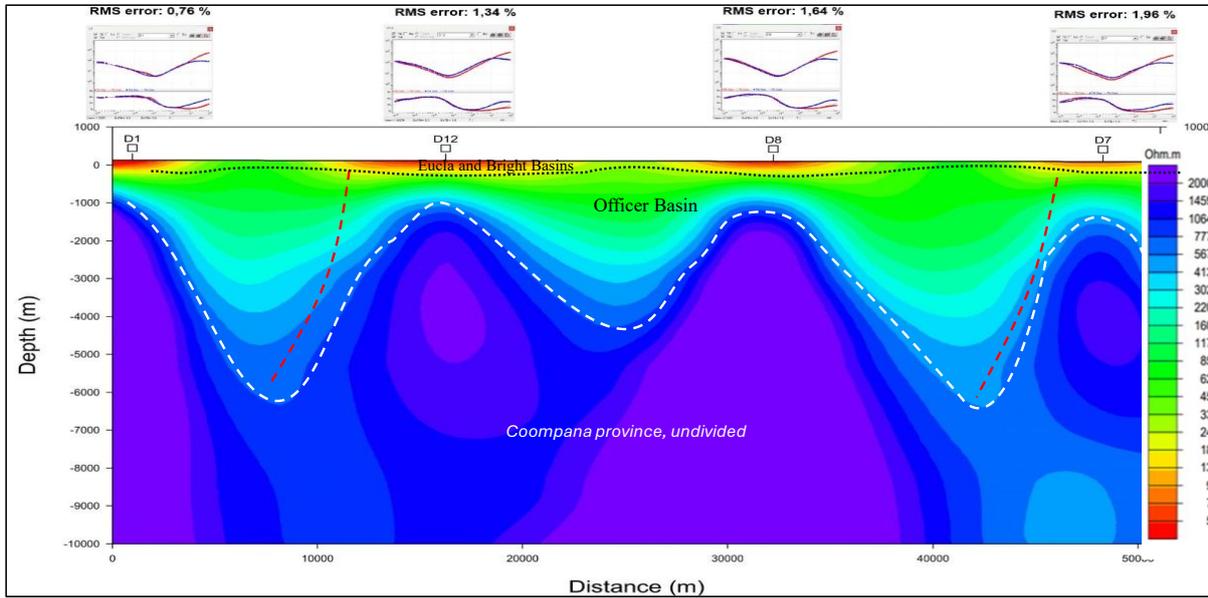

Figure 7. 2D inversion line 2 at Nullarbor.

The 2D resistivity model in line 2 also shows the low to intermediate resistivity uptown 6000 m and bedrock (basement) is identified as intrusive rock, granite, at >1000 m. In line 2, geological structures in the form of suspected shear zone with a maximum depth of 6000 m. The Eucla and

Bright Basins consisting of sediment and Vulcanic rocks including Tun formation (Czi) are identified at varying depths ranging from surface to several hundred meters. Sedimentary rock, Claystone, are identified to be at varying depths ranging from 500 m to approximately 6000 m.

Bedrock (basement) is identified as intrusive rock, which is granite is at varying depths with a maximum depth range of > 1000 m. In addition, a line 3 (not include in this research) has similar lithology (shown in crossline, Figure 8).

Figure 8 is a visualization of crossline modeling for all lines, where crosslines are created with the aim of seeing the continuity of resistivity in each subsurface model for each line.
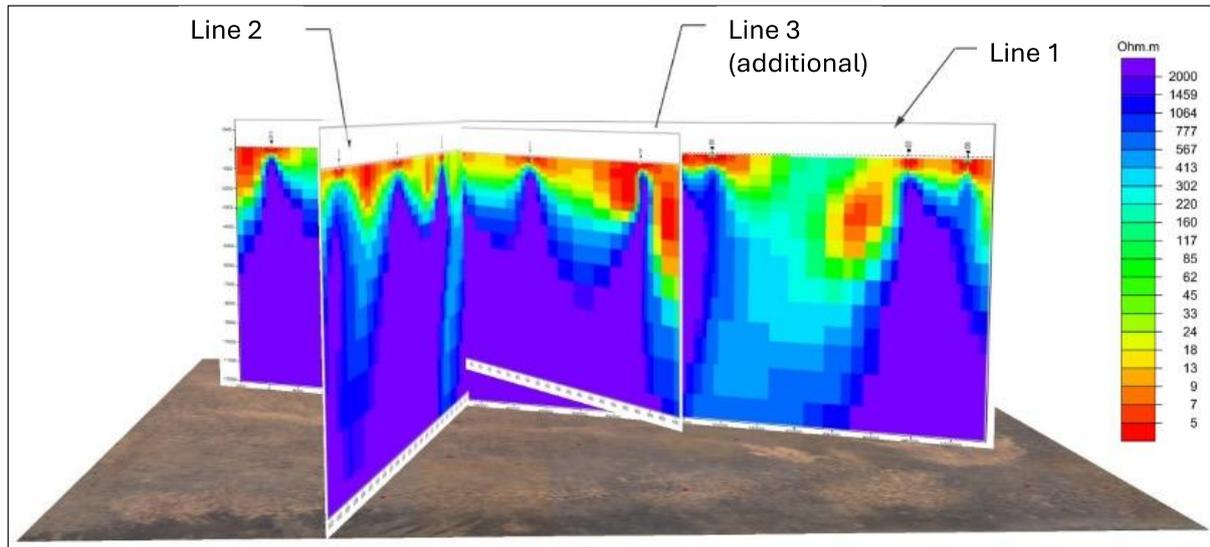
Figure 8. Crossline visualization of all lines.

In the first layer, the most conductive layer is interpreted as limestone, the second layer as claystone, and the basement is the most resistive layer interpreted as granite. Based on the correlation between previous research and the crossline line model, a geological structure in the form of a shear zone with a maximum depth of up to 6 km was identified. The existence of this SZ is believed to be the cause of the earthquake and has the potential to form other structural geological features. Based on the correlation between the geologic map and the crossline model of the line, one main structure of Miocene to Pliocene age in the Quaternary period was identified (Yang et al., 2022). The crossline in Figure shows the continuation of the geological structure at the intersection at point D1 and reflects the consistency of the rock layers and the continuity of the lithologic types of all the passes.

The existence of this geological structure is confirmed based on previous research by Yang et al. (2022) who interpreted that there are geological structures in Nullarbor. According to Yang et al. (2022) there are geological structures in the form of thrust faults and folds that have poor resolution because the MT method has a low resolution of 10^{-5} to 10^{4}. Earthquakes that occur repeatedly on the same surface on a fault can extend the fault through lateral propagation and accumulate displacements that can be measured through fault or fold analysis. In Australia, about 2900 individual surface traces combine into about 350 tectonic surface features (faults and folds) mostly caused by thrust fault displacement (Sellmann et al., 2022).

Conclusion

Based on the results of this study, it can be concluded that the phase tensor analysis states that the dimensional structure in the study area has 1D characteristics at shallow depth, 2D at medium depth, and 2D at deep depth. In the study area, 2D data is dominant at intermediate depths with the N5ºE displayed in geoelectric direction.

This geoelectric direction is used to rotate the MT data and minimize errors in 2D inversion modeling. The MT data shows rock layers consisting of the Eucla Basin, which is composed of sedimentary and volcanic rocks, has a resistivity value below 10 Ωm. In contrast, the Officer Basin, which contains sedimentary rock, exhibits higher resistivity values ranging from 10 to approximately 300 Ωm. Additionally, a highly resistive layer with values between 300 and 2000 Ωm is believed to represent the upper crust in the central Coompana Province, particularly along a corridor rich in granite. The 2D inversion cross section shows a resistivity contrast that is identified as a geological structure in form of shear zone with a depth until 6000 m depth, confirming the presence of significant geological structures. The study demonstrates the efficacy of combining phase tensor analysis and 2D MT inversion for delineating subsurface lithology and structure in the region.

Acknowledgements

Author Contribution

Sarah Manurung conceptualized the research, data processing and analysis, and write the manuscript and. Andri Yadi Paembonan supervised the research, provided critical guidance throughout the research process, and contributed to the interpretation of the results. Selvi Misnia Irawati provided expertise in data analysis, contributed to data interpretation, and provided valuable insights during manuscript preparation. All authors contributed to the writing and revision of the manuscript.

Conflict of Interest

The authors declare no conflict of interest.

References

Akbar, S., Setyawan, A., Yulianto, T., Baroek, M. C., & Ramadhan, I. (2020). Analisis Dimensionalitas Data Magnetotellurik Lapangan Panas Bumi "SA" Berdasarkan Metode Tensor Fase. *Berkala Fisika*, 23(2), 49–55. https://ejournal.undip.ac.id/index.php/berkala_fisika/article/view/30623

Arisbaya, I., Wijanarko, E., Warsa, W., Sumintadireja, P., Sudrajat, Y., Handayani, L., Mukti, M. M., & Grandis, H. (2023). Magnetotellurics (MT) and gravity study of a possible active fault in southern Garut, West Java, Indonesia. *International Journal of Geophysics*, 4482074. https://doi.org/10.1155/2023/4482074

Barajas-Olalde, C., Adams, D. C., Curcio, A., Davydycheva, S., Klapperich, R. J., Martinez, Y., Paembonan, A. Y., Peck, W. D., Strack, K., & Soupios, P. (2023). Application of electromagnetic methods for reservoir monitoring with emphasis on carbon capture, utilization, and storage. *Minerals*, 13(10), 1308; https://doi.org/10.3390/min13101308

Bravo-Osuna, A. G., Gómez-Treviño, E., Cortés-Arroyo, O. J., Delgadillo-Jauregui, N. F., & Arellano-Castro, R. F. (2021). Reframing the magnetotelluric phase tensor for monitoring applications: improved accuracy and precision in strike determinations. *Earth Planets Space*, 73, 34. https://doi.org/10.1186/s40623-021-01354-y

Chang, P.-Y., Amania, H. H., Fikri, A., Puntu, J. M., Lin, D.-J., Kuo, C.-H., Wang, C.-Y., & Chang, W.-Y.

(2023). Probing shallow subsurface structures in the arc-continent collision suture zone near Hualien in Eastern Taiwan with magnetotelluric methods. *Geoscience Letters*, 10(1). 29. https://doi.org/10.1186/s40562-023-00283-w

Cowley, W. (2020). *Geological Map South Australia.* Department for Energy and Mining.

Geological Survey of Western Australia. (2017). *Geological interpretation of the Madura and Coompana Provinces along the Eucla-Gawler seismic and magnetotelluric line 13GA-EG1.* Geological Survey of Western Australia.

Guo, R., Li, M., Yang, F., Xu, S., & Abubakar, A. (2020). Application of supervised descent method for 2D magnetotelluric data inversion. *Geophysics*, 85(4), WA53–WA65. https://doi.org/10.1190/geo2019-0409.1

Heath, P., Gouthas, G., Irvine, J., Krapf, C., & Dutch, R. (2018). Microgravity surveys on the Nullarbor. *ASEG Extended Abstracts*, 2018(1), 1–7. https://doi.org/10.1071/ASEG2018abM3_2H

Heath, P. (2017). Quantifying the differences between gravity reduction techniques. *Exploration Geophysics*, 49(5), 735–743. https://doi.org/10.1071/eg17094

Hou, B., Keeling, J., Reid, A., Petts, A., & Stoian, L. (2022). *Eucla Basin and peripheral paleovalleys, Report Book 2022/00011.* Adelaide: Department for Energy and Mining, South Australia

Hu, P., Heslop, D., Rossel, R. A. V., Roberts, A. P., & Zhao, X. (2019). Continental-scale magnetic properties of surficial Australian soils. *Earth-Science Reviews*, 203, 103028. https://doi.org/10.1016/j.earscirev.2019.103028

Irawati, S. M., Paembonan, A. Y., & Fernanda, L. (2024). Aplikasi Tensor Fase Data Magnetotellurik untuk Pemodelan Panas Bumi The Geysers, California dan Dikorelasikan dengan Data Gaya Berat. *Jurnal Geosains Dan Teknologi*, 6(3), 186–202. https://doi.org/10.14710/jgt.6.3.2023.186-202

Jiang, W., McAlpine, S., Duan, J., Dutch, R., & Pawley, M. (2017). *Cover Thickness Estimates in the Coompana Province, South Australia.* Canberra: Commonwealth of Australia (Geoscience Australia)

Kirkby, A. L., Zhang, F., Peacock, J., Hassan, R., & Duan, J. (2019). The MTPy software package for magnetotelluric data analysis and visualisation. *The Journal of Open-Source Software*, 4(37), 1358. https://doi.org/10.21105/joss.01358

Lin, W., Yang, B., Han, B., & Hu, X. (2023). A Review of Subsurface Electrical Conductivity Anomalies in Magnetotelluric Imaging. *Sensors*, 23(4), 1803. https://doi.org/10.3390/s23041803

Marwan, M., Yanis, M., Zahratunnisa, Z., Idroes, R., Nugraha, G. S., Dharma, D. B., Susilo, A., Saputra, D., Suriadi, S., & Paembonan, A. Y. (2022). Geothermal reservoir depth of Seulawah Agam Volcano estimated from 1D Magnetotelluric. *Journal of Applied Engineering Science*, 20(3), 754–764. http://dx.doi.org/10.5937/jaes0-36077

Maswah, F., Suryantini, S., Srigutomo, W., Fajri, R. J., Pratama, A. B., & Pratomo, P. M. (2021). Magnetotelluric data analysis using phase tensor and tipper strike to determine geoelectrical strike in "DKH" geothermal field. *IOP Conference Series Earth and Environmental Science*, 732(1),

012014. https://doi.org/10.1088/1755-1315/732/1/012014

Pawley, M. J., Dutch, R. A., & Wise, T. W. (2020). The relationship between crustal architecture, deformation, and magmatism in the Coompana Province, Australia. *Tectonics*, 39(12), e2019TC005593. https://doi.org/10.1029/2019TC005593

Pertiwi, T. B., Daud, Y., & Fahmi, F. (2023). Investigation of geological structure using magnetotelluric and gravity data optimization on non-volcanic geothermal, Bora, Centre of Sulawesi. *Journal of Geoscience, Engineering, Environment, and Technology*, 8(2), 103–111. https://doi.org/10.25299/jgeet.2023.8.02-2.13876

Scheib, A., Morris, P., Murdie, R., & Piane, C. D. (2016). A passive seismic approach to estimating the thickness of sedimentary cover on the Nullarbor Plain. *Western Australia. Australian Journal of Earth Sciences*, 63(5), 583–598. https://doi.org/10.1080/08120099.2016.1233455

Sellmann, S., Quigley, M., Duffy, B., Yang, H., & Clark, D. (2022). Fault geometry and slip rates from the Nullarbor and Roe Plains of south-central Australia: Insights into the spatial and temporal characteristics of intraplate seismicity. *Earth Surface Processes and Landforms*, 48(2), 350–370. https://doi.org/10.1002/esp.5490

Webb, J. A., & James, J. M. (2006). *Karst evolution of the Nullarbor Plain, Australia.* Geological Society of America. https://doi.org/10.1130/2006.2404(07)

Yang, H., Sellmann, S., & Quigley, M. (2022). Fluid-Enhanced Neotectonic Faulting in the Cratonic Lithosphere of the Nullarbor Plain in South-Central Australia. *Geophysical Research Letters*, 49(4), e2022GL099155. https://doi.org/10.1029/2022GL099155